

# FACTS - DG Coordination in an Integrated Transmission & Distribution Network (IT & DN)

A. A. Sadiq<sup>a\*</sup>, I. A. Damari<sup>b</sup>, M. Buhari<sup>c</sup>, S. S. Adamu<sup>c</sup>, J. G. Ambafi<sup>a</sup>

<sup>a</sup> Department of Electrical and Electronic Engineering, School of Electrical Engineering and Technology, Federal University of Technology Minna, Nigeria.

<sup>b</sup> Department of Electrical Engineering, Federal Polytechnic Daura, Nigeria

<sup>c</sup> Department of Electrical Engineering, Faculty of Engineering, Bayero University Kano, Nigeria

[ahmad.abubakar@futminna.edu.ng](mailto:ahmad.abubakar@futminna.edu.ng)

doi: 10.21608/jeatsa.2025.427794

Received 21-8-2024

Revised \*\*\*\* \*\* \*\*

Accepted: 1-11-2024

Published: Jan-2025

Copyright © 2021 by author(s) and  
Journal Of Engineering Advances And Technolog  
Sustainable Applications  
This work is licensed under the Creative  
Commons Attribution International  
License (CC BY 4.0).

<http://creativecommons.org/licenses/by/4.0/>



Open Access

Print ISSN: 3062-5629

Online ISSN: 3062-5637

**Abstract-** To support improved performance and a sustainable power supply amid growing demand, modern power grids increasingly integrate Flexible AC Transmission Systems (FACTS) together with Distributed Generation (DG). However, planning studies often treat FACTS and DG independently, overlooking their mutual influence on system optimization. The work herein presents a bi-level optimization strategy designed to coordinate DG and FACTS for enhancing ATC, minimizing active losses, and reducing deviations in voltages. The methodology involves two optimizations: the Inner and Outer (IO and OO). The inner deploys a hybrid of the active flow Performance Index and PSO to plan Flexible AC Transmission Systems while Outer leverages Multiple objective variants of particle swarm optimization (MOPSO) to plan DG within a case study distribution network. The test network includes a distribution and transmission components, specifically using the Western Systems Coordinating Council's 9-bus system and the IEEE 16-node model. PV and PQ DG models are synchronized with two types of FACTS, TCSC and SSSC. Findings indicate notable ATC improvements, particularly with TCSC - PQ<sub>DG</sub> and SSSC - PQ<sub>DG</sub> combinations, and the Pareto front curves reveal a non-linear trend, where ATC gains plateau beyond a certain maximum value as the Pareto slope nears zero.

**Keywords-** DG, FACTS, FACTS-DG Coordination, Transmission and Distribution network, PSO.

## I. INTRODUCTION

AC transmission systems popularly known as FACTS are critical in promoting sustainable energy delivery by enhancing power flow control, increasing transfer capacity, damping oscillations, and enabling flexible grid management [1], [2]. Also, recent distribution systems are accommodating significant capacities of Distributed Generation (DG). Consequently, maintaining active flows and voltages within limits requires either upgrades of infrastructure or injection of VARS from FACTS [3].

The increased penetration of renewable energy-based DG is driven by the de-carbonisation of the power supply chain [4]. However, the penetration of DG, particularly into the DN, significantly affects DN planning and operation, making network planning difficult [5]. One of the challenges of modern DN is the accurate understanding of their interaction with the installed compensating devices, such as FACTS in large power grids [6]. Advantages offered by FACTS devices to power grids depends on optimal location, sizing, and their coordination with other system devices, especially at the DN level, which accommodates load.

While they have become common components of the recent power grid, in planning studies, FACTS devices and Distributed Generation (DG) are frequently implemented at high and low voltage levels, respectively, but often without properly coordinating their effects. In DG planning, it is typically assumed that the transmission network—with or without FACTS—are firm, overlooking the influence of FACTS control operations. Conversely, FACTS planning often models the distribution network as a passive, fixed-power load. However, the rise of active distribution networks, driven by greater DG integration, challenges this

assumption. In such settings, improved active power demand without coordinated of components such as FACTS and DG can lead to degraded power system performance. [7], [8]. The magnitude and composite nature of the power grid, the prerogative of the unbundled companies, and the need for steadfast process of distinctly planned transmission and distribution networks also institute the factors in scheduling and processes of the power grid as a one entity [9]. With the growing integration of Distributed Generation (DG) and controllable devices like FACTS in Distribution Networks (DN), traditional methods that treat transmission and distribution systems as separate entities have become less effective. [10]. This paper presents as a test network a synthetic combined transmission and distribution network model, which combines low and high current networks.

## II. RELATED WORK

Although the coordination of multiple FACTS like TCSC, SVC and UPFC was presented by [11], while the works in [12], [13] present synchronization of multiple FACTS for ATC enhancement. The coordination, however, ignores real power generation, which often characterises DG to meet increased load demand. To take care of DGs in [14], the focus of optimized DN planning with solar power and DSTACOM was the extension of a non-dominant sorted genetic algorithm (NSGA II); hence the improvement overlooks the impacts of the DGs and DSTACOM on several purposes. Similarly, the work in [5] concludes that while DG penetration in power systems causes stability issues, UPFC, compared to SVC, is better for eliminating transients and improving voltage profile. Also, UPFC was deployed for stability improvement of Microgrids (MG) in [15]. The work in [3] acknowledged that voltage,

thermal, and fault current are the limitations to DG penetration and demonstrated the capabilities of STATCOM, SSSC and UPFC in relieving network constraints, thereby improving DG penetration. Additionally, [16] analysed the VAR mismatch resulting from integrating DFIG-based DG units on low voltage networks. It was demonstrated that TCSC boosts the collapse boundary, reduce voltage variation to Var and expand voltage stabilities. In [17], a method to synchronize SVC and OLTC with wind-based DG-induced disturbances was developed to minimise counteraction. From the works in [11], [12], [13], [14], [15], [16], [17], although FACTs and DGs were considered simultaneously, the impacts caused by interactions and consequently their coordination were not adequately considered.

Accordingly, to enhance active flows in high voltage lines, the synchronization of DG and UPFC is documented by [18]. In that work, apparent power flows increase, together with the active power transmitted with UPFC and wind DG coordination. Nevertheless, the degree of interactions amongst were unclear. Similarly, influence of DG in coordination with SVC is discussed in [19]. Among the issues discussed in [20] is the combination of wind plants for combined high voltage expansion planning and TCSC site. The findings indicate that optimal placement and configuration of a TCSC can substantially lower load curtailment and enhance the utilization of wind energy sources. In [19], [20], while the coordination and investigation of DGs and SVC performance indices were studied, the test network was limited to only DN.

FACTS DG coordination in a restructured framework entails distinct objectives due to the prerogatives of the TSO and DSO; hence, a multi-level optimization approach. A two-level outline is presented in [21] for the best collaboration of energy hubs and low voltage networks. In the study, the objectives of minimizing Distribution Network (DN) operating costs and individual energy hub costs are addressed as upper- and lower-level targets. However, combining these multiple objectives into a single one can diminish the interactions between different energy sources. In this work, a two-level optimization strategy for synchronizing FACTS and DG is presented, thereby improving ATC, reduce active losses, and minimize deviations in voltage. Specifically, this work presents the results of the coordination of two series FACTS devices—TCSC and SSSC—with DG.

### III. METHODOLOGY

For the FACTS–DG coordination an approach called bi-level optimisation is developed, which is made up of the Inner Optimization (IO) and Outer Optimisation (OO). As shown in Figure 1, IO implements the mix of PSO and real power flow (PI – PSO) to optimally plan FACTS [1]. At the same time, the OO targets DG at DN and implements a Multiple variant of PSO called MOPSO.



Figure (1): Experimental system under study Bi-level optimisation for FACTS - DG Coordination

#### A. The Inner Optimisation (PI – PSO)

The comprehensive description of combined PI – PSO is presented in [1], [12], [13]. The position of a particle is expressed by equation (1), such that  $\lambda$  and  $\eta$  indicates the line and capacity of FACTS, each. Also, the position as well as velocity of equations (2) to (3) are augmented by equation (4), for a candidate location having an m-dimension vector, equations (4) express the position update in PI – PSO [1].

$$X_i^k = [\lambda_i^k; \eta_i^k] \quad (1)$$

$$X_i^{k+1} = X_i^k + V_i^{k+1} \quad (2)$$

$$V_i^{k+1} = \alpha V_i^k + c_1 \text{rand}(P_{best}^k - X_i^k) + c_2 \text{rand}(G_{best}^k - X_i^k) \quad (3)$$

$$X_i^{k+1} = \begin{cases} X_i^{k+1}(\lambda_i) & \text{if } \lambda_i^{k+1} \in \square \\ \square (\text{randperm}(m,1)) & \text{if } \lambda_i^{k+1} \notin \square \\ X_i^{k+1}(\eta_i) & \text{for } \eta_i \in \square \end{cases} \quad (4)$$

Using the parameterized continuous load flow, ATC is evaluated at the maximum loading parameter [1], as described in equation (5).

$$\text{Max}_{(\lambda, \lambda_k, V_{se}, \delta_{se})} \left\{ ATC = \sum_{i \in \text{sink}} P_L^i(\lambda_{lim}) - \sum_{i \in \text{sink}} P_L^i(\lambda_0) \right\} \quad (5)$$

$$f(x, \lambda) = 0 \quad (6)$$

$$0 \leq \lambda \leq \lambda_{limited} \quad (7)$$

$$P_{min} \leq P_g \leq P_{max} \quad (8)$$

$$Q_{min} \leq Q_g \leq Q_{max} \quad (9)$$

$$S_{ij} \leq S_{ij}^{rated} \quad (10)$$

$$V_i^{min} \leq V_i \leq V_i^{max} \quad (11)$$

$$X_{FACTS}^{min} \leq X_{FACTS} \leq X_{FACTS}^{max} \quad (12)$$

and angle of voltages. In equations (7) to (11) the terms  $\lambda_{limited}$ ,  $P_g$ ,  $Q_g$ ,  $S_{ij}$ , and  $V_i$  are loading parameter, real, reactive, apparent power flows, and voltage magnitude, respectively. FACTS capacities are considered as constraints described by equation (12), such that the percentage recompense of TCSC is within  $-0.8 \leq X_{TCSC} \leq 0.2$  and injection by SSSC is within  $0 \leq X_{SSSC}^{Vse} \leq 0.1$ . The model which represent TCSC and SSSC as apparent injection are discussed by [12].

#### A. The Outer Optimisation (MOPSO)

Flexible AC system in TN aims to maximise ATC, while DG targets efficient power delivery by minimising actual real loss ( $P_{loss}$ ) and voltages away from ideal ( $V_D$ ) at DN. Thus, the two objectives of DG planning in DN are parallel and conflict with the ATC enhancement with FACTS at TN. Hence, the approach adopts a multiple objective variant of PSO referred to as MOPSO. The MOPSO provides a set of distinct and non-dominated Pareto results. To coordinate DG in DN with the existing Transmission Network (TN) based FACTS, the combined transmission distribution system is the test network.

#### B. Test Network: combined Transmission and Distribution Network

The test network represents the transmission section by the Western System Coordinating Council (WSCC) - 9 buses while the distribution section is represented by IEEE 16 buses network. As depicted in Figure 2, the test is built in MATPOWER software and visualised and confirmed using the Steady-State AC Network Visualization for MATPOWER case data.

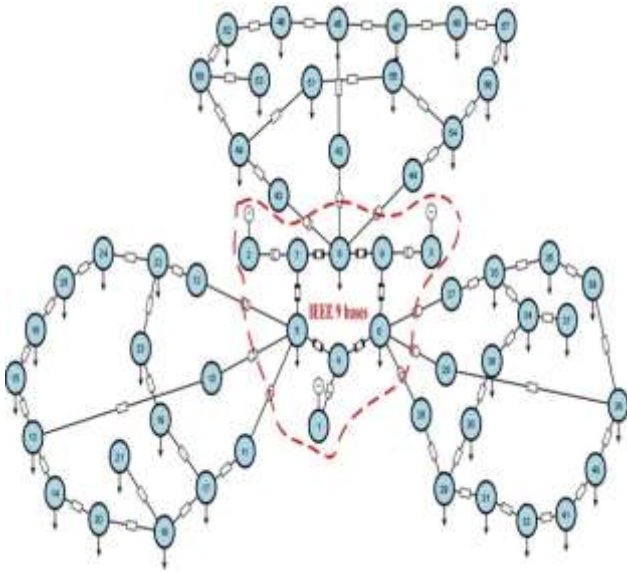


Figure (2): Integrated Trans. and Dist. Network (iT & DN).

### IV PROBLEM FORMULATION OF FACTS – DG COORDINATION

Since the objectives for the DG and FACTS coordination involves improving the ATC and reducing the active loss and deviation of voltages from ideal, the optimization needs to be transformed into the same front as either maximisation or minimisation. Equation (13) defines the minimisation problem design of FACTS –DG synchronization for 3 purposes.

$$\min f(x; \lambda) = [f_1(x; \lambda); f_2(x; \lambda); f_3(x; \lambda)] \quad (1)$$

Accordingly, equation (13) is constrained to the constraint's equations (6) to (12) for FACTS placement and additional constraints equations (14) and (15), which limit the maximum apparent power of DG sizes to 2/3 of the load in DN [22], [23]. Two types of DG (PV and PQ models) [4] were separately synchronized with FACTS such as TCSC and SSSC, respectively.

$$0 \leq \gamma_{dg}^p \leq 0.75P_{load}^{dn} \quad (2)$$

$$-0.75Q_{load}^{dn} \leq \gamma_{dg}^q \leq 0.75Q_{load}^{dn} \quad (3)$$

#### A. Evaluation of Fitness in MOPSO

In equation (16) represent the comprehensive fitness vector of objectives, ATC, active loss and deviations in voltage for the FACTSDG coordination using MOPSO.

$$\vec{f}(x, \lambda) = \begin{cases} -ATC = -Equation(5) \\ P^{loss} = \sum_{k=1}^{nl} g_k [V_i^2 + V_j^2 - 2V_i V_j \cos(\delta_i - \delta_j)] \\ V_D = \sum_{i=1}^{nb} |1 - V_i| \end{cases} \quad (4)$$

In equation (16), opposing the ATC term of equation (5) transforms the entire fitness vector into a minimisation problem. A run of CPF with the initial or updated particle's position implement each transaction. Equations (17) and (18) describe the vector elements that model FACTS and DG sizes.

$$X_{facts} = \begin{cases} -jx_k; & -0.2 \leq x_k \leq 0.8 \\ V_{se}, \delta_{se}; & 0 \leq V_{se} \leq 0.1, -\pi \leq \delta_{se} \leq \pi \end{cases} \quad (5)$$

$$X_{DG} = \begin{cases} \gamma_{dg}^p; PV \text{ model}, & 0 \leq \gamma_{dg}^p \leq 0.75P_{load}^{dn} \\ \gamma_{dg}^p, +\gamma_{dg}^q; PQ \text{ model}, & 0 \leq \gamma_{dg}^q \leq 0.75Q_{load}^{dn} \end{cases} \quad (6)$$

#### B. Dominance Determination in MOPSO

For a general minimisation problem, a vector  $\vec{f}_i(x, \lambda)$  of objectives produced by a particle with the position  $Pos_i^o$

dominates any other vector  $\vec{f}_j(x, \lambda)$  of objectives produced by another particle  $Pos_j^o$ , scientifically expressed as  $\vec{f}_i(x, \lambda) \prec \vec{f}_j(x, \lambda)$ , according to the equation (19).

$$\begin{aligned} \forall i \in \{1, 2, 3\} : f_i(x, \lambda) < f_j(x, \lambda) \text{ and} \\ \exists i \in \{1, 2, 3\} : f_i(x, \lambda) < f_j(x, \lambda) \end{aligned} \quad (1)$$

Due to the conflicting nature of the fitness vector terms of the equation (16), MOPSO retains all non-dominated results by equation (19) in a storage [24], [25]. The storage, also known as the repository, is limited to 100 non-dominated solution members to ensure the diversity of the Pareto front. The repository members are updated during each iteration with a pressure equal to the selection pressure.

#### A. Selection of Leader

In the case of contradictory objectives, a single universal best solution is often intricate. From the storage of non-dominated solutions, a leader is designated to guide other particles towards better regions within the search space. Here, selection of leader is based on Roulette wheel technique.

Thus, the chance of selecting the  $i^{\text{th}}$  solution from the storage is given by equation (20).  $P_r$  is described by equation (21), where  $\tau$  denoted pressure of selecting a particle.  $N$  is the number of particles in the storage.

$$P^i = \frac{P_r}{\sum_{i \in 1} P_r} \quad (2)$$

$$P_r = e^{-\tau N} \quad (3)$$

The cumulative chance of picking particles from the storage is given by equation (22), while  $r_i \in (0, 1)$  of equation (23) is a uniformly generated between 0 and 1.

$$q_i = \sum_{i=1}^N P^i, \text{ for } i=1 \text{ to } N \quad (4)$$

$$r_i = rand() \quad (5)$$

Using equations (22) and (23), equation (24) describes the criteria to obtain the catalog of the chosen participant of the storage to serve as a leader.

$$leader_{index} = find(r_i \leq q_i) \quad (6)$$

With the personal best update, the leader selection, the position and velocity in the OO are updated in the same as equations (2) and (3).

#### B. Mutation Operation in MOPSO

The mutation operator is applied to any  $j^{\text{th}}$  randomly selected element of the particle position of the equation according to equation (25) [26, 27, 28], such that  $\psi$  is a randomly chosen between the minor bound  $X_{lb}$  and higher bound  $X_{ub}$  of the control variable, which includes the size of

FACTS as well as location and size of DG selected for mutation.

$$Pos_i^{new}(j) = \psi(X_{lb}(j) - X_{ub}(j)) \quad (7)$$

In addition to limitations imposed on the minor and greater bound of the control variables,  $X_{lb}$  the greater bound  $X_{ub}$  is described by equation (26), where  $Pos^k(j)$  is the position of the particle at  $k^{\text{th}}$  iteration and equation (27) defines  $\Delta x$ .

$$\begin{cases} X_{lb} = Pos^k(j) - \Delta x \\ X_{ub} = Pos^k(j) + \Delta x \end{cases} \quad (8)$$

$$\Delta x = \xi(X^{\max} - X^{\min}) \quad (9)$$

Equation (27)  $X^{\min}$  and  $X^{\max}$  are vectors stipulating the least and extreme limits of decision variables of the particle position  $Pos^k(j)$ . In contrast, equation (28) describes the mutation scaling factor  $\xi$  [26]. Where  $it$ ,  $Max\_it$ , and  $mu_r$  are the current iteration, maximum iteration and mutation rate, respectively.

$$\xi = \left( 1 - \frac{it-1}{Max\_it-1} \right)^{\left( \frac{1}{mu_r} \right)} \quad (10)$$

Figure 3 depicts the flow chart of the two-level approach for FACTS DG coordination. Plotting the Pareto front of ATC versus active loss and ATC versus deviation in voltage, establishes the correlation among the various objectives.

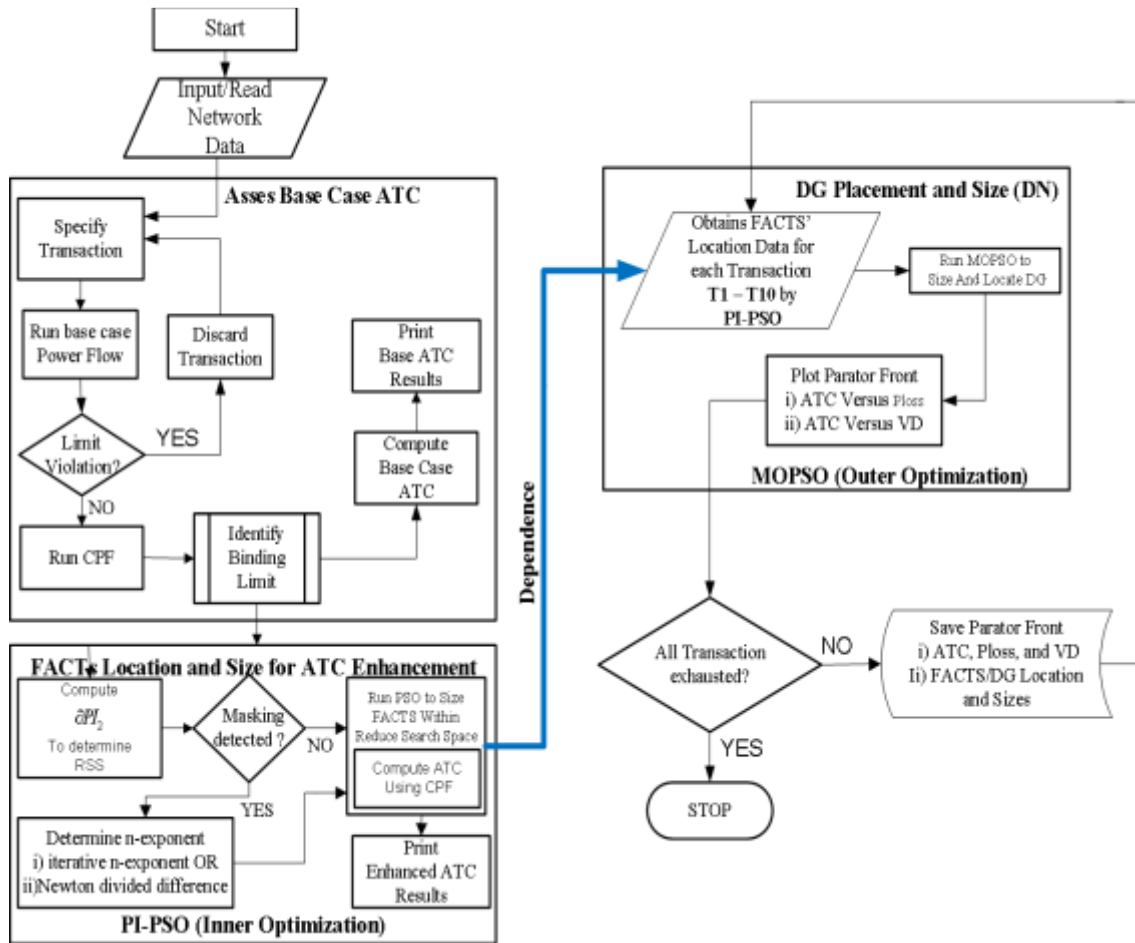


Figure (3): Flow Chart of the Bi-level optimisation

Table (1): ATC values with TCSC - DG coordination

| Trans. ID.     | Transactions |      | ATC [MW]  |                  |                  | TCSC - $PV_{DG}$ Solution |           |             |                  | TCSC - $PQ_{DG}$ Solution |           |             |                        |
|----------------|--------------|------|-----------|------------------|------------------|---------------------------|-----------|-------------|------------------|---------------------------|-----------|-------------|------------------------|
|                | Source       | Sink | TCSC Only | TCSC - $PV_{DG}$ | TCSC - $PQ_{DG}$ | Plos [MW]                 | VD [p.u.] | TCSC % Comp | $DG_{Size}$ [MW] | Plos [MW]                 | VD [p.u.] | TCSC % Comp | $DG_{Size}$ [MW, MVar] |
| T <sub>A</sub> | 1 & 3        | 5    | 155       | 169              | 196              | 6.2                       | 3.8       | 80          | 4.0              | 4.4                       | 3.1       | 80          | [11.24&13]             |
| T <sub>B</sub> | 1 & 2        | 5&8  | 153       | 154              | 155              | 4.7                       | 3.0       | 49          | 8.7              | 4.7                       | 2.4       | 47          | [0&13]                 |
| T <sub>C</sub> | 1,2 & 3      | 5&6  | 172       | 172              | 174              | 4.8                       | 3.8       | 80          | 10.2             | 4.6                       | 3.3       | 69          | [0&12.95]              |
| T <sub>D</sub> | 1,2 & 3      | 6&8  | 178       | 179              | 183              | 5.0                       | 4.2       | 26          | 21.5             | 4.9                       | 3.8       | 41          | [0&12.99]              |

#### IV. RESULTS AND DISCUSSION

Different scenarios of power transactions were considered, as outlined in Table I. The power transfers consist of bilateral (T-A) and multilateral (T-B, T-C and T-D) transactions with the transfer directions described by the source and sink columns in Table (1).

A participant of the non-dominated result is chosen as optimum conciliation of the three objectives based on two-level norms. Firstly, the ATC improvement is accorded precedence, such that all storages' members with bigger ATC than FACTS constitute a feasible result. The second condition is based on domination, and a storage member with greater than two higher objectives related to FACTS only equally constitutes a feasible result. Accordingly, an optimal solution

is obtained from the list of feasible solutions by applying the first-level norms again. The best coordination results for TCSC-DG and SSSC - DG are recorded in Table (1) and Table (2), respectively.

Table (1) shows that higher ATC for T-A is attained under TCSC placed at line 8 with 80% compensation. DG was best planed at node 18 with active and VAR injections of 11.24 MW and 13 MVar, each.

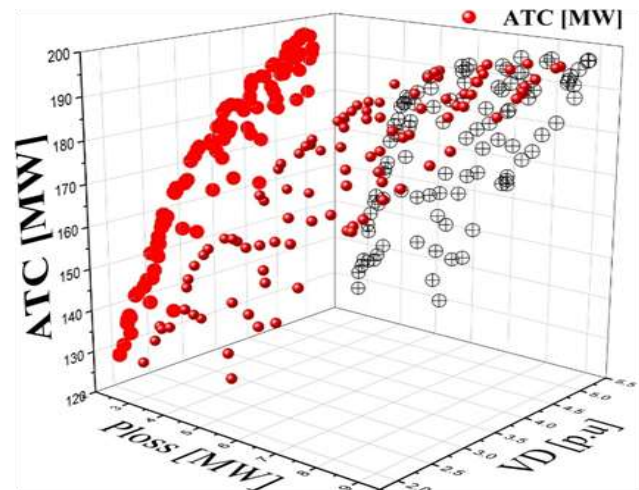
In Table (2), the best ATC for T-C is achieved with SSSC optimally placed at line 3 having series injection  $V_{se}$  of  $0.094 p.u. \angle 2.14 rad$ , with best DG location at node 13 having active and VAR of 5.59 MW and 13 MVar each.

Table (2): ATC values with SSSC - DG coordination.

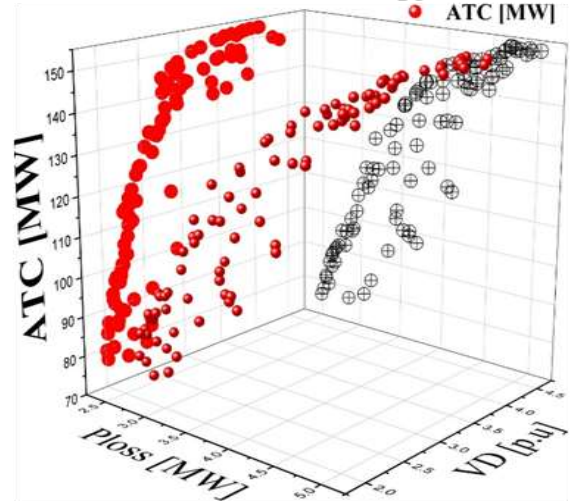
| Trans. ID. | ATC [MW]  |                  |                  | SSSC - $PV_{DG}$ Solution |           |                 |                |                  | SSSC - $PQ_{DG}$ Solution |           |                 |                |                        |
|------------|-----------|------------------|------------------|---------------------------|-----------|-----------------|----------------|------------------|---------------------------|-----------|-----------------|----------------|------------------------|
|            | SSSC Only | SSSC - $PV_{DG}$ | SSSC - $PQ_{DG}$ | Ploss [MW]                | VD [p.u.] | $V_{se}$ [p.u.] | $d_{se}$ [rad] | $DG_{Size}$ [MW] | Ploss [MW]                | VD [p.u.] | $V_{se}$ [p.u.] | $d_{se}$ [rad] | $DG_{Size}$ [MW, MVAr] |
| T-A        | 148       | 156              | 191              | 5.7                       | 4.0       | 0.07            | 3.1            | 3.8              | 5.8                       | 4.9       | 0.10            | 1.4            | [5.15&12.86]           |
| T-B        | 152       | 153              | 154              | 4.9                       | 4.1       | 0.10            | 2.5            | 21.5             | 4.9                       | 3.6       | 0.10            | 2.6            | [0&13]                 |
| T-C        | 141       | 178              | 195              | 4.2                       | 4.3       | 0.08            | 2.1            | 21.5             | 4.0                       | 3.8       | 0.094           | 2.1            | [5.59&13]              |
| T-D        | 177       | 178              | 180              | 5.0                       | 4.4       | 0.06            | 1.1            | 19.8             | 4.8                       | 3.8       | 0.066           | 0.4            | [0&13]                 |

The Pareto front plots for transactions T-A and T-B are depicted in Figures (4) and (5). The distinct and non-dominated front of TCSC - DG and SSSC - DG is demonstrated for both PV and PQ models of DG. The portions of the Pareto front plots provide further relationship between objectives.

Consequently, from the combined 3D Pareto front plots of Figures (4) and (5), the Pareto plot's portions of ATC versus to active power loss (Ploss) and ATC versus voltage deviation (VD) are obtained and as shown in Figures (6) and (7).

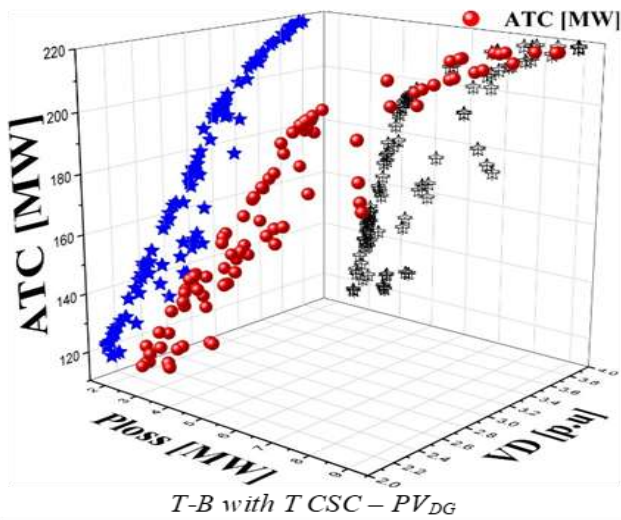


T-B with SSSC -  $PV_{DG}$

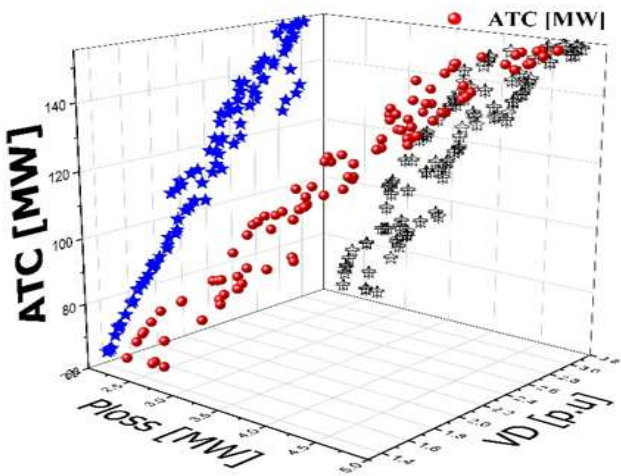


(b) T-A with SSSC -  $PQ_{DG}$

Figure (5): Pareto Front for SSSC - DG Coordination.

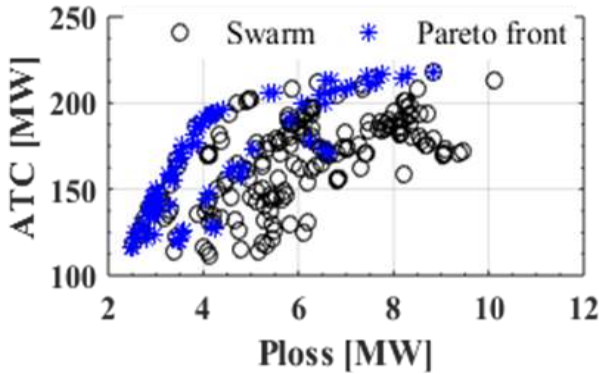


T-B with TCSC -  $PV_{DG}$

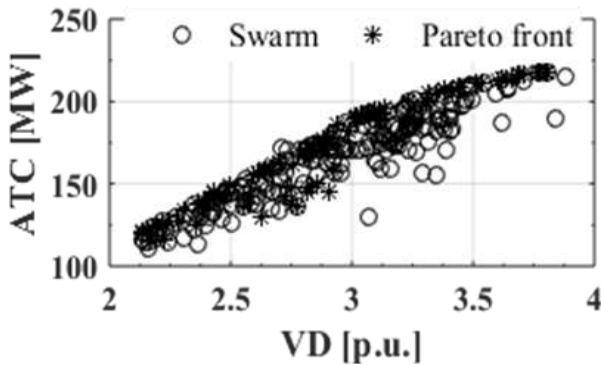


(b) T-A with TCSC -  $PQ_{DG}$

Figure (4): Pareto Front for TCSC - DG Coordination.

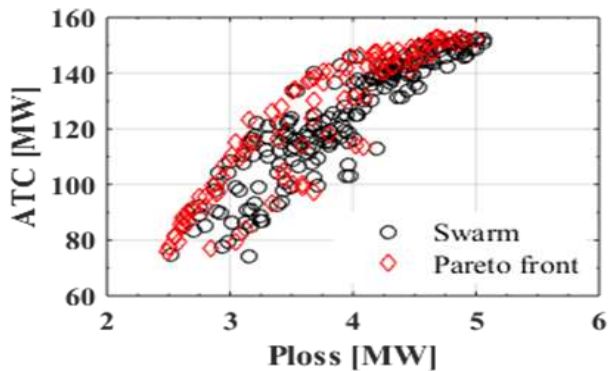


(a) ATC versus Ploss (TCSC – PQ<sub>DG</sub>) for T-A

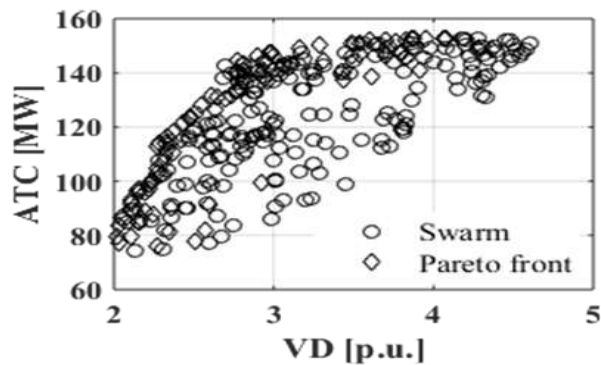


(b) ATC versus VD (TCSC-PQ<sub>DG</sub>) for T-A

Figure (6): Portions of Pareto plot for transactions T-A



(a) ATC versus Ploss (SSSC – PV<sub>DG</sub>) for T-B



(a) ATC versus VD (SSSC – PV<sub>DG</sub>) for T-B

Figure (7): Portions of Pareto plot for transactions T-B

For the TCSC – PQ<sub>DG</sub> coordination, observe from Figures 6a and 6b improvement of ATC to about 200 MW at Ploss and VD of about 4.49 MW and 3.2 p. u., separately. The gradient of the Pareto front in Figure (6)b is nearly persistent. In contrast, the parabolic-like shapes of Figure (6)a depict a non-linear gradient imminent zero after an ATC of 200 MW and imply an increasing Ploss with approximately constant ATC. Similarly, Figures (7)a and (7)b depicts a non-linear gradient imminent zero above an ATC of 152 MW.

## V. CONCLUSIONS

In this work, a novel bi-level approach to coordinate FACTS devices (TCSC and SSSC) with different types of DG (PV and PQ) is presented. The proposed framework addresses multiple objectives, including maximizing ATC, minimizing power losses, and maintaining voltage quality in both transmission and distribution systems. The Pareto front analysis illustrates the trade-offs between these objectives, with a diminishing marginal return on ATC beyond a certain threshold. The TCSC-PQ<sub>DG</sub> and SSSC-PQ<sub>DG</sub> combinations exhibit the best performance in terms of ATC and loss reduction, while also effectively managing voltage deviations.

## VI. REFERENCES

- [1] A. A. Sadiq, S. S. Adamu, and M. Buhari, Available transfer capability enhancement with FACTS using hybrid PI-PSO, Turkish J. Electr. Eng. Comput. Sci., vol. 27, no. 4, pp. 2881-2897, 2019.
- [2] X. Zhang, K. Tomsovic, and A. Dimitrovski, Optimal allocation of series FACTS devices in large-scale systems, IET Gener. Transm. Distrib., vol. 12, no. 8, pp. 1889-1896, 2018.
- [3] J. M. Bloemink and T. C. Green, Benefits of distribution-level power electronics for supporting distributed generation growth, IEEE Trans. Power Deliv., vol. 28, no. 2, pp. 911-919, 2013.
- [4] A. A. Sadiq, S. S. Adamu, and M. Buhari, Optimal distributed generation planning in distribution networks: A comparison of transmission network models with FACTS, Eng. Sci. Technol. an Int. J., vol. 22, no. 1, pp. 33-46, 2019.
- [5] P. K. Pandey and B. Bag, A comparative study on UPFC and SVC towards voltage profile improvement of a grid-connected distributed generation system, in 2015 International Conference on Energy, Power and Environment: Towards Sustainable Growth, ICEPE 2015, pp. 15, 2015.
- [6] Y. Feng, S. Wang, C. Xue, Y. Cao, J. Wu, and H. Li, Flexible coordinated optimal operation model of source-grid-load-storage in the intelligent distribution network, Proc. - 2020 5th Asia Conf. Power Electr. Eng. ACPEE 2020, pp. 223-236, 2020.

- [7] H. Gerard, E. I. Rivero, and D. Six, Coordination between transmission and distribution system operators in the electricity sector: A conceptual framework, *Util. Policy*, vol. 50, pp. 4048, 2018.
- [8] A. G. Givisiez, K. Petrou, and L. F. Ochoa, A Review on TSO-DSO Coordination Models and Solution Techniques, *Electr. Power Syst. Res.*, vol. 189, no. October 2019, p. 106659, 2020.
- [9] H. Jain, K. Rahimi, A. Tbaileh, R. P. Broadwater, A. K. Jain, and M. Dilek, Integrated Transmission & Distribution System Modeling and Analysis: Need & Advantages, in 2016 IEEE Power and Energy Society General Meeting (PESGM), pp. 15, 2016.
- [10] L. Shiguang, Y. Ting, P. Tianjiao, M. Jie, and S. Fan, Coordinated optimisation control method of transmission and distribution network, in Asia-Pacific Power and Energy Engineering Conference, APPEEC, pp. 22152219, 2016.
- [11] M. Nadeem et al., Optimal Placement, Sizing and Coordination of FACTS Devices in Transmission Network Using Whale Optimisation Algorithm, *Energies*, vol. 13, no. 753, pp. 124, 2020.
- [12] A. A. Sadiq, M. Buhari, S. S. Adamu, and H. Musa, Coordination of multi-type FACTS for available transfer capability enhancement using PI-PSO, *IET Gener. Transm. Distrib.*, vol. 14, no. 21, 2020.
- [13] A. A. Sadiq, S. S. Adamu, and M. Buhari, Multi-Type FACTS Location and Coordination using PI-PSO for Transfer Capability Improvement, in IEEE PES/IAS PowerAfrica Conference: Power Economics and Energy Innovation in Africa, PowerAfrica 2019, pp. 662667, 2019.
- [14] S. R. Ghatak, S. Sannigrahi, and P. Acharjee, Optimised planning of power distribution network with solar energy, Battery storage and DSTATCOM: A multi-objective approach, in 2018 IEEE International Conference on Power Electronics, Drives and Energy Systems (PEDES), pp. 16, 2018.
- [15] H. Saberi, S. Mehraeen, and B. Wang, Stability Improvement of Microgrids Using a Novel Reduced UPFC Structure via Non-linear Optimal Control, in 2018 IEEE Applied Power Electronics Conference and Exposition (APEC), pp. 32943300, 2018.
- [16] T. F. Orchi, M. J. Hossain, H. R. Pota, and M. S. Rahman, Impact of distributed generation and series compensation on the distribution network, in Proceedings of the 2013 IEEE 8th Conference on Industrial Electronics and Applications, ICIEA 2013, pp. 854859, 2013.
- [17] Ravi and R. Raman, Coordination between SVC and OLTC for voltage control in Wind Energy Conversion System, *Int. Res. J. Eng. Technol.*, vol. 3, no. 10, pp. 482485, 2016.
- [18] M. Farsadi, F. M. Shahir, D. Nazarpour, and F. N. Heris, Analysing of coordinate operational of UPFC based on matrix converter and wind turbine generator under unbalanced load, in ELECO 2015 - 9th International Conference on Electrical and Electronics Engineering, pp. 525529, 2016.
- [19] B. Singh, V. Mukherjee, and P. Tiwari, GA-based Optimisation for optimally placed and properly coordinated control of distributed generations and Static Var Compensator in distribution networks, *Energy Reports*, vol. 5, pp. 926959, 2019
- [20] F. Ugranli and E. Karatepe, Coordinated TCSC Allocation and Network Reinforcements Planning with Wind Power, *IEEE Trans. Sustain. Energy*, vol. 8, no. 4, pp. 16941705, 2017.
- [21] A. Mirzapour-Kamanaj, M. Majidi, K. Zare, and R. Kazemzadeh, Optimal strategic coordination of distribution networks and interconnected energy hubs: A linear multi-follower bi-level optimisation model, *Int. J. Electr. Power Energy Syst.*, vol. 119, no. January, p. 105925, 2020.
- [22] E. S. Ali, S. M. A. Elazim, and A. Y. Abdelaziz, Ant Lion Optimization Algorithm for Optimal Location and Sizing of Renewable Distributed Generations, *Renew. Energy*, vol. 101, pp. 13111324, 2017.
- [23] S. A. Chithradevi, L. Lakshminarasimman, and R. Balamurugan, Stud Krill Herd Algorithm for Multiple DG Placement and Sizing in a Radial Distribution System, *Eng. Sci. Technol. an Int. J.*, vol. 20, no. 2, pp. 748759, 2017.
- [24] A. Britto and A. Pozo, I-MOPSO: A Suitable PSO Algorithm for ManyObjective Optimization, in Proceedings - Brazilian Symposium on Neural Networks, 2012, pp. 166171.
- [25] P. K. Tripathi, S. Bandyopadhyay, and S. K. Pal, Multi-Objective Particle Swarm Optimization with Time-Variant Inertia and Acceleration Coefficients, *Inf. Sci. (Ny)*, vol. 177, no. 22, pp. 50335049, 2007.
- [26] H. Farahmand, M. Rashidinejad, A. Mousavi, A. A. Gharaveisi, M. R. Irving, and G. A. Taylor, Hybrid Mutation Particle Swarm Optimisation Method for Available Transfer Capability Enhancement, *Int. J. Electr. Power Energy Syst.*, vol. 42, no. 1, pp. 240249, 2012.
- [27] Sadiq, A. A., Buhari, M., Ambafi, J. G., Adamu, S. S., & Nwohu, M. N. (2023). Contingency constrained TCSC and DG coordination in an integrated transmission and distribution network: A multi-objective approach. *E-Prime - Advances in Electrical Engineering, Electronics and Energy*, 4(March), 100156.  
<https://doi.org/10.1016/j.j.prime.2023.100156>
- [28] Sadiq, A. A., Yusuf, L., Buhari, M., Adamu, S. S., & Ambafi, J. G. (2024). Coordination of Flexible Alternating Current Transmission Systems and Distributed Generation in a Synthetic Co-simulation of Transmission and Distribution Network. *Turkish Journal of Electrical Power and Energy Systems*, epub ahead.  
<https://doi.org/10.5152/tepes.2024.23026>